BIODIVERSITAS
Volume 26, Number 8, August 2025
Pages: 3711-3721

ISSN: 1412-033X
E-ISSN: 2085-4722
DOI: 10.13057/biodiv/d260805

Wing cell shape variation in malaria vector species of the *Anopheles barbirostris* complex and closely related species (Diptera: Culicidae)

SEDTHAPONG LAOJUN[1], ARINA ABDULLOH[1], ATIPORN SAEUNG[2], TANAWAT CHAIPHONGPACHARA[1,♥]

[1]Department of Public Health and Health Promotion, College of Allied Health Sciences, Suan Sunandha Rajabhat University. 111/1-3 Rama 2 Street, Samut Songkhram 75000, Thailand. Tel./fax.: +66-347-73905, ♥email: tanawat.ch@ssru.ac.th

[2]Parasitology and Entomology Research Cluster (PERC), Department of Parasitology, Faculty of Medicine, Chiang Mai University. 2 Suthep, Mueang, Chiang Mai 50200, Thailand

Manuscript received: 4 July 2025. Revision accepted: 3 August 2025.

Abstract. *Laojun S, Abdulloh A, Saeung A, Chaiphongpachara T. 2025. Wing cell shape variation in malaria vector species of the* Anopheles barbirostris *complex and closely related species (Diptera: Culicidae). Biodiversitas 26: 3711-3721.* Several *Anopheles* species, including members of the *An. barbirostris* complex, contribute significantly to malaria transmission in Thailand. Accurate species identification is hindered by high morphological similarity, reducing the effectiveness of traditional taxonomy. This study examined wing cell shape variation in three complex members (*An. dissidens*, *An. saeungae*, *An. wejchoochotei*) and their sister species *An. hodgkini* using an outline-based geometric morphometric approach. A total of 136 specimens—*An. dissidens* (n = 30), *An. saeungae* (n = 30), *An. wejchoochotei* (n = 46), and *An. hodgkini* (n = 30)—were analyzed. Eleven wing cells were digitized, and shape variables extracted via Elliptic Fourier Analysis were evaluated with discriminant analysis to assess interspecific variation. Significant shape differences ($p < 0.05$) were detected for most species pairs and wing cells. *Anopheles hodgkini* exhibited the greatest morphological divergence, especially in the first basal, marginal, and second posterior cells. In contrast, some comparisons within the complex, such as between *An. dissidens* and *An. wejchoochotei* in the anal cell, were not significant ($p > 0.05$). Cross-validated reclassification accuracy ranged from 44.12% (anal cell) to 58.09% (second posterior cell). These results demonstrate that wing cell shape analysis can support discrimination among morphologically similar malaria vectors. Geometric morphometrics offers a cost-effective, rapid method for assessing morphological variation, providing valuable taxonomic resolution and aiding detection of cryptic *Anopheles* species. While GM alone may not achieve high classification accuracy, it generates complementary morphological evidence to molecular diagnostics. In resource-limited public health settings, GM can serve as a preliminary identification tool, enhancing vector surveillance by enabling more precise mapping of high-risk transmission zones. Accurate differentiation of *Anopheles* species is essential for effective malaria control, as species vary in vectorial capacity, behavior, and ecology, informing targeted and efficient intervention strategies.

Keywords: Malaria vectors, mosquitoes, outline-based geometric morphometric approach, species identification, wing cells

INTRODUCTION

The *Anopheles barbirostris* complex, classified under the Barbirostris Subgroup of the Myzorhynchus Series within the subgenus *Anopheles*, consists of cryptic mosquito species that are morphologically indistinguishable. Eight taxa are formally described, six of which inhabit Thailand: *An. barbirostris*, *An. campestris*, *An. dissidens*, *An. donaldi*, *An. saeungae*, and *An. wejchoochotei* (Taai and Harbach 2015; Somboon et al. 2023). The remaining species, *An. sarpangensis* (Somboon et al. 2024) and *An. vanderwulpi* (Townson et al. 2013), occur in Bhutan and Indonesia, respectively. *Anopheles donaldi* was recently added based on phylogenetic evidence and shared morphological features across life stages (Somboon et al. 2023, 2024). This complex has a broad Oriental distribution, from Timor and the Indonesian archipelagos to Guam, mainland Southeast Asia, southern China, and parts of South Asia. Several species are linked to malaria transmission, including outbreaks in Thailand (Taai and Harbach 2015; Udom et al. 2021).

Malaria, caused by *Plasmodium* parasites transmitted via *Anopheles* bites, remains a major public health threat (Nguyen et al. 2023; Rotejanaprasert et al. 2024). Symptoms range from mild fever to severe multi-organ failure, influenced by parasite species, host immunity, and access to treatment. In Thailand, cases have declined, but transmission persists in border provinces (Parker et al. 2015; Tananchai et al. 2019). Multiple *Anopheles* species act as vectors, including members of the *An. barbirostris* complex. Species A3, once suspected to be a new complex member, was reclassified as *An. hodgkini*, a sister species (Somboon et al. 2023).

Anopheles campestris and *An. wejchoochotei* are more anthropophilic and implicated in malaria or filarial transmission, whereas others are zoophilic and not confirmed as vectors (Harrison and Scanlon 1975; Taai and Harbach 2015). *Anopheles wejchoochotei* is widespread in Thailand and often co-occurs with *An. dissidens* and *An. saeungae* (Taai and Harbach 2015; Chaiphongpachara et al. 2022b). Accurate species identification is essential for vector control but is hindered by morphological similarity. Traditional keys often identify only to group level, e.g., by

a tuft of black scales on sternum VII (Rattanarithikul et al. 2006), limiting precision in areas where cryptic species with differing vector capacities co-exist (Taai and Harbach 2015). This constraint necessitates alternative diagnostic approaches that can provide finer taxonomic resolution.

Recent studies suggest wing cells can help distinguish vector species in Thailand (Laojun et al. 2024; Changbunjong et al. 2025). Wing cells—enclosed regions formed by vein intersections—vary in shape, size, and arrangement among species, providing potential species-specific traits.

Geometric Morphometrics (GM) quantitatively analyzes size and shape and is widely applied for insect identification (Dujardin et al. 2014; Wilke et al. 2016; Dujardin and Dujardin 2019; de Souza et al. 2020). GM has proven effective for vectors such as sand flies, stable flies, fleas, and mosquitoes (Sauer et al. 2022; Weluwanarak et al. 2024; Chotelersak et al. 2024; Lozano-Sardaneta et al. 2025). In mosquitoes, it has successfully resolved cryptic taxa in the Dirus and Minimus complexes (Chatpiyaphat et al. 2021; Chaiphongpachara et al. 2022a). GM is cost-effective, requiring only standard lab equipment and allowing rapid processing—advantageous for damaged field specimens. Its application is particularly relevant in tropical regions where resources for molecular diagnostics may be limited.

Wings are often analyzed due to their durability and taxonomic value. Landmark-based GM uses specific vein intersections, while outline-based GM is suited for curved or continuous structures lacking clear landmarks (Dujardin et al. 2014). In outline-based GM, pseudo landmarks along wing contours capture shape variation without predefined anatomical points. This study applies outline-based GM to wing cell contours to assess its taxonomic potential alongside molecular methods. Wing shape reflects both ecological pressures and genetic control, with minor differences indicating genetic divergence (Bellin et al. 2021; Oliveira-Christe et al. 2021). In cryptic complexes, where external traits fail, wing shape can reliably indicate evolutionary relationships. Thus, GM of wing cells may bridge the gap between morphological ambiguity and genetic distinctiveness in vector taxonomy.

Accurate identification is vital, as cryptic species may differ in transmission potential, biting behavior, host choice, and breeding ecology (Jeon et al. 2023). Misidentification risks ineffective control. Wing shape GM not only improves taxonomy but also aids malaria epidemiology by mapping vector ranges, refining risk assessments, and informing targeted interventions.

This study examines wing cell shape variation in *An. dissidens*, *An. saeungae*, and *An. wejchoochotei*, plus *An. hodgkini*, using outline-based GM. We hypothesize this method can detect subtle differences sufficient for species discrimination. The outcomes aim to enhance species identification accuracy, strengthen surveillance systems, and ultimately contribute to more efficient vector control in malaria-endemic zones.

MATERIALS AND METHODS

Anopheles collection

Anopheles mosquitoes were collected over a 14-night period between August and October 2022 at three locations in Thailand, previously reported as sites of coexistence of the three target species: *An. dissidens, An. saeungae*, and *An. wejchoochotei*. The selected sites were Kanchanaburi (14°07'47.4"N, 98°59'46.0"E), Narathiwat (6°21'19.3"N, 101°53'41.6"E), and Trat (12°28'19.7"N, 102°40'10.3"E) (Rattanarithikul et al. 2006; Taai and Harbach 2015) (Figure 1).

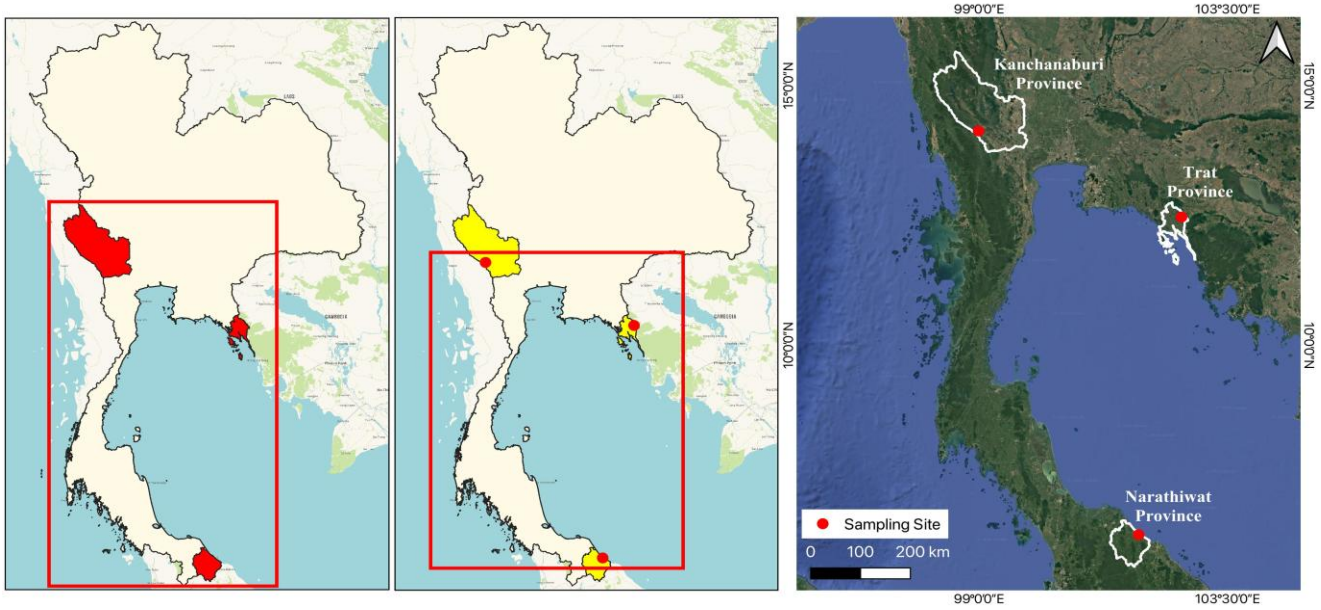

Figure 1. Geographical map showing the locations of three mosquito sampling sites in Thailand: Kanchanaburi Province, Narathiwat Province, and Trat Province. The map was created using publicly available data from the USGS National Map Viewer (http://viewer.nationalmap. gov/viewer/), which is in the public domain

Collections were conducted during Thailand's monsoon season, a period that typically supports increased mosquito proliferation due to favorable environmental conditions. At each site, eight BG-Pro CDC-style traps (BioGents, Regensburg, Germany) were deployed to capture mosquitoes. To increase trapping efficiency, each trap was baited with a BG-Lure cartridge (BioGents) and supplemented with dry ice as a source of carbon dioxide. Each trap was suspended at an elevation of approximately 1.5 meters above the ground and placed at a distance of approximately 10 meters from residential dwellings that had previously reported malaria cases. One trap was allocated per household to ensure a standardized sampling effort across all locations. Trapping was conducted nightly from 6:00 PM to 6:00 AM. Each morning, captured mosquitoes were euthanized by placing the sample bags in dry ice containers for 20 minutes at -20°C. After the 10-day collection period, all specimens were transported to the laboratory for both molecular and morphological identification, followed by further analyses.

Species identification

Due to the high degree of morphological similarity among species within the *An. barbirostris* complex, accurate identification based solely on external morphological features is not feasible. Consequently, initial morphological screening was employed to assign specimens to the *An. barbirostris* complex, followed by molecular techniques for definitive species-level identification. Adult female mosquitoes presumed to belong to this complex were examined under a Nikon SMZ800N stereo microscope (Nikon Corp., Tokyo, Japan) using standard morphological keys for Thai *Anopheles* species (Rattanarithikul et al. 2006). After preliminary identification, each mosquito was placed into a separate 1.5 mL microcentrifuge tube to preserve sample integrity for downstream DNA analysis.

To molecularly confirm species-level identification, genomic DNA was extracted from legs of morphologically screened specimens. The DNA extraction was performed using the FavorPrep™ Tissue Genomic DNA Extraction Mini Kit (Favorgen Biotech, Ping-Tung, Taiwan), following the manufacturer's protocol. Molecular species identification was conducted using a multiplex PCR assay targeting diagnostic regions of the cytochrome *c* oxidase subunit I (*COI*) gene specific to the *An. barbirostris* complex, following the protocol described by Wilai et al (2020). The primer set used in this study comprises multiple primers, as shown in Table 1. Each Polymerase Chain Reaction (PCR) was prepared in a total volume of 20 µL. The reaction mixture comprised 1 µL of extracted genomic DNA, a standard 1× concentration of PCR buffer, magnesium chloride ($MgCl_2$) at a final concentration of 3 mM, 0.2 mM of each deoxynucleotide triphosphate (dNTP), 0.2 µM of each primer specific to target species, and 0.4 units of Platinum Taq DNA polymerase (Invitrogen, Carlsbad, California, USA). The remaining volume was adjusted with nuclease-free water. Each PCR run included a negative control (nuclease-free water) and a positive control (DNA from previously validated reference specimens). PCR products were electrophoretic ally separated on a 2% agarose gel stained with Midori Green (Nippon Gene, Tokyo, Japan). DNA bands were observed under ultraviolet illumination. Species identification was based on the presence of distinct DNA amplicon sizes corresponding to each member of the *An. barbirostris* complex (Table 1).

Wing preparation, digitization, and repeatability.

Each specimen's right wing was carefully dissected from the thorax and mounted on a microscope slide using Hoyer's medium as the mounting agent. A coverslip was applied to secure the wing in place for imaging. To ensure a clear outline of digitization, wing scales were gently removed using fine needles during the mounting process. The prepared slides were left undisturbed at room temperature for approximately seven days to allow the medium to harden and stabilize the wings. High-resolution images of the mounted wings were obtained using a digital imaging system integrated with a Nikon SMZ800N stereomicroscope (Nikon Corporation, Tokyo, Japan). These images were then used to digitize the contours of 11 specific wing cells: the marginal cell, the first and second submarginal cells, the first through fourth posterior cells, the first and second basal cells, the anal cell, and the auxiliary cell (Figure 2). All cell outlines were digitized using an outline-based Geometric Morphometric (GM) approach. The same specimens were used for all cell analyses to maintain consistency across comparisons.

Table 1. Primer set for multiplex PCR targeting the *COI* gene used in this study for species identification within the *An. barbirostris* complex and *An. hodgkini* (formerly *An. barbirostris* species A3; currently recognized as a distinct species outside the complex)

***Anopheles* species**	**Primer name**	**Direction**	**Sequence (5′ → 3′)**	**Product size (bp)**
An. barbirostris s.s.	BARA4	Forward	AAT AGT AGG AAC TTC TTT ATG A	706
An. dissidens	BARA1	Forward	ATT ACT ACT GTT ATT AAT ATA GGA	238
An. saeungae	BARA2	Forward	TTA GGT CAC CCA GGA GCA	611
An. wejchoochotei	BARWEJ	Forward	GAT TTG GAA ACT GAT TAC TG	502
An. hodgkini	BARA3	Forward	CGG AAC TGG ATG AAC TGT A	365
Universal reverse	HCO2198	Reverse	TAA ACT TCA GGG TGA CCA AAA AAT CA	-
Long GC tail sequence (This primer was combined with the BARA4 primer specific to *An. barbirostris* s.s. to generate a larger PCR product)	-	-	GCG GGC AGG GCG GCG GGG GCG GGG CC;	-

Note: The primer set used in this study was based on the design by Wilai et al. (2020)

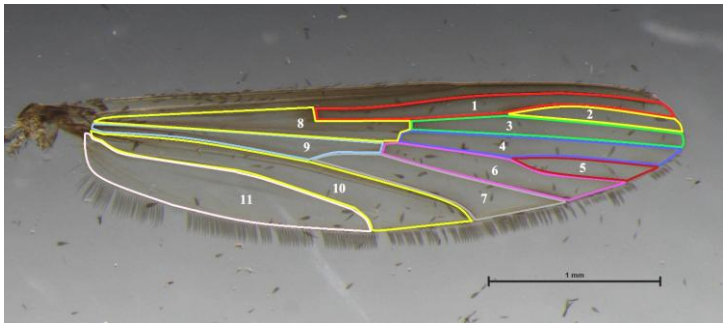

Figure 2. Eleven wing cells used for outline-based geometric morphometric analysis, comprising: 1: The marginal cell, 2: The first submarginal cell, 3: The second submarginal cell, 4: The first posterior cell, 5: The second posterior cell, 6: The third posterior cell, 7: The fourth posterior cell, 8: The first basal cell, 9: The second basal cell, 10: The anal cell, 11: The auxiliary cell. The outline of each wing cell was defined using pseudo landmarks, allowing for shape analysis without relying on anatomical vein intersections

To evaluate the accuracy of digitization, Procrustes Analysis of Variance (ANOVA) was conducted following Arnqvist and Mårtensson (1998). For each wing cell, 10 randomly selected wings were digitized twice by the same observer. The analysis yielded a repeatability (R) score of 91% for shape, indicating high consistency and showing that only 9% of the variation observed was due to measurement error.

Wing cell shape analyses

Sample sizes were determined based on the total number of high-quality wing specimens available. Each species group consisted of at least 30 individuals. To evaluate interspecific differences in wing cell shape and to define shape variables, elliptic Fourier analysis (EFA) was employed. This method decomposes the wing outline into a series of sine and cosine functions, referred to as harmonics, each represented by four numerical coefficients. The first harmonic is used to standardize the data, rendering it invariant to size, orientation, and starting point. Following this normalization, only the remaining coefficients, particularly those reflecting shape features such as the wing's width-to-length ratio, were retained for further analysis (Santillán-Guayasamín et al. 2017). Elliptic Fourier analysis offers considerable analytical flexibility, as it does not necessitate the use of anatomically homologous landmarks or equidistant coordinate points among samples. This characteristic makes it particularly suitable for capturing the complex contours of biological outlines. Due to the potentially high number of Fourier coefficients needed to describe closed shapes fully, dimensionality reduction was performed using principal component analysis (PCA). This multivariate approach transforms the original correlated coefficients into a reduced set of orthogonal principal components (PCs) that retain the most salient aspects of shape variability. These PCs were subsequently utilized as input variables in comparative statistical analyses.

To assess interspecific shape variation, the resulting shape variables were subjected to Discriminant Analysis (DA). Group separation was visualized using factor maps based on the first and second Discriminant Functions (DF1 and DF2). Morphological divergence among species was quantified using Mahalanobis distances for all pairwise comparisons. A non-parametric permutation test with 1,000 iterations was used to assess the statistical significance of wing shape differences. For multiple pairwise comparisons, Bonferroni correction was applied, and *p*-values less than 0.05 were considered statistically significant. To evaluate the discriminatory power of wing cell shape for species classification, a leave-one-out cross-validation procedure (cross-validated classification) was employed. Each specimen was sequentially excluded from the dataset and assigned to the nearest group centroid in multivariate morphometric space based on Mahalanobis distance.

Software

All morphometric analyses were conducted using the XYOM platform (XY Online Morphometrics), version 2, (Dujardin and Dujardin 2019). The Digitization module was used to trace wing outlines, while the Classification module facilitated shape analysis, including discriminant analysis, Mahalanobis distance calculations, and pairwise comparisons. The Miscellaneous module was employed to evaluate repeatability.

Ethical statement

All experimental protocols involving animals were reviewed and approved by the Institutional Animal Care and Use Committee (IACUC) of Suan Sunandha Rajabhat University, Thailand, under protocol number IACUC 64-007/2021. The study was carried out in strict adherence to institutional guidelines governing the ethical treatment of animals in research.

RESULTS AND DISCUSSION

Molecular identification

A total of 136 mosquito specimens collected from field sites were initially classified morphologically as members of the *An. barbirostris* complex. These specimens were subsequently subjected to species-level confirmation using a multiplex PCR assay. Molecular results revealed the presence of four distinct species. Three of them—*An. dissidens* (30 specimens), *An. saeungae* (30 specimens),

and *An. wejchoochotei* (46 specimens)—were confirmed as members of the *An. barbirostris* complex, while the remaining 30 specimens were identified as *An. hodgkini* (Table 2).

Wing cell shape variation

Superimposed mean wing cell shapes (Figures 3 and 4) illustrate morphological differences among *An. dissidens, An. saeungae*, *An. wejchoochotei*, and *An. hodgkini*. Although the overall shapes appear broadly similar across species, distinct differences, particularly in the curvature and orientation of specific wing cells, are clearly observable. Factor maps generated from DA further reveal subtle yet consistent shape variation among the four species. Despite considerable overlap in the distribution of individual data points, clear separation is evident in the centroid positions of each group (Figures 5 and 6), underscoring interspecific morphological divergence.

Figure 4 demonstrates species-level shape variation across 11 wing cells. While none of the species form completely discrete clusters in discriminant space, their mean shape positions remain distinguishable. Of all examined cells, the second posterior cell displayed the most pronounced separation, with *An. hodgkini* occupying a distinctly different region of morphospace—particularly in the first submarginal and second posterior cells. This supports the interpretation that *An. hodgkini*, though taxonomically related to the *An. barbirostris* complex is morphologically more divergent, consistent with its unique ecological and genetic attributes. By contrast, *An. dissidens, An. saeungae*, and *An. wejchoochotei* exhibited greater overlap, especially in the anal cell, suggesting lower levels of morphological differentiation. This pattern may reflect shared evolutionary constraints or ecological convergence, as these species are often sympatric and may inhabit similar environments or display overlapping behaviors. The biological relevance of these wing shape variations warrants further investigation through ecological, behavioral, and genetic studies.

Pairwise comparisons using Mahalanobis distances revealed statistically significant differences ($p<0.05$) in wing cell shape among most species pairs across nearly all wing cells (Table 3). Notably, *An. hodgkini* consistently demonstrated the greatest divergence from the other taxa, with particularly high Mahalanobis distances observed in comparisons with *An. dissidens* for the first basal cell (3.017; $p<0.05$), marginal cell (3.029; $p<0.05$), and second posterior cell (3.171; $p<0.05$). While *An. dissidens, An. saeungae*, and *An. wejchoochotei* exhibited significant differences in most wing cells; a few pairwise comparisons did not reach statistical significance. Specifically, no significant differences were observed between *An. dissidens* and *An. saeungae* in the first submarginal cell (1.605; $p>0.05$), between *An. dissidens* and *An. wejchoochotei* in the anal cell (1.582; $p>0.05$), and again between *An. dissidens* and *An. saeungae* in the auxiliary cell (1.794; $p>0.05$).

Cross-validated classification

Based on cross-validated reclassification, overall accuracy across all wing cells ranged from 44.12% to 58.09% (Table 4). The anal cell produced the lowest overall classification performance (44.12%), indicating that it offers limited taxonomic resolution for distinguishing species based on wing cell shape. In contrast, the second posterior cell yielded the highest overall reclassification accuracy (58.09%). Among the four species, *An. hodgkini* achieved the highest individual reclassification rates in several cells, most notably in the marginal cell (66.67%), second posterior cell (66.67%), and auxiliary cell (63.33%). Conversely, *An. saeungae* generally exhibited lower classification performance, with the lowest accuracy observed in the first posterior cell (30%).

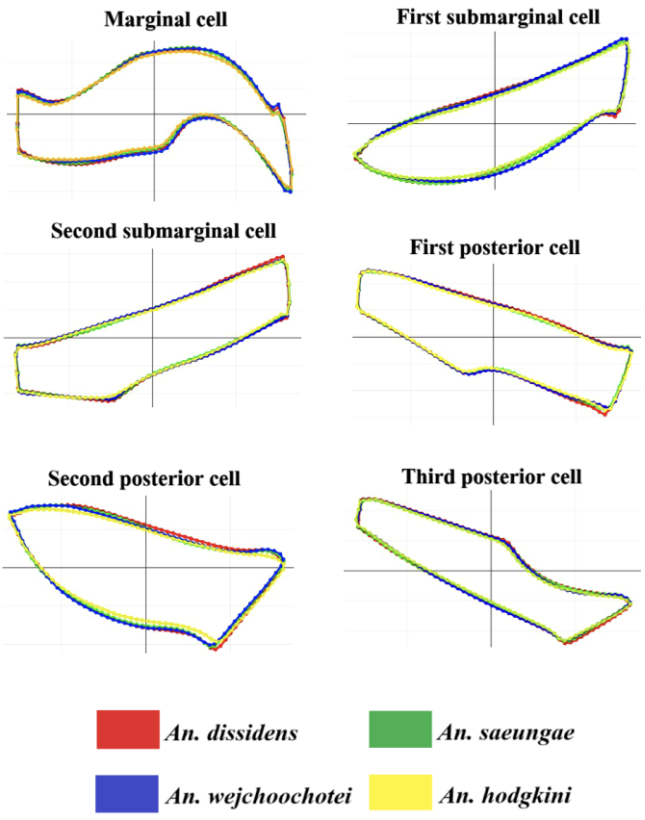

Figure 3. Superimposed mean wing cell shapes illustrating interspecific differences among *An. dissidens, An. saeungae*, *An. wejchoochotei,* and *An. hodgkini* across six wing cells: the marginal cell, first and second submarginal cells, and first to third posterior cells. Each colored outline represents the mean shape of a species: red for *An. dissidens*, green for *An. saeungae*, blue for *An. wejchoochotei*, and yellow for *An. hodgkini*. The degree of overlap between the outlines reflects interspecific variation in wing cell shape. Although all cells display some degree of morphological divergence, the differences are generally modest

Table 2. Number of mosquitoes in the *Anopheles barbirostris* complex and sister species used for geometric morphometric analysis, as confirmed by the multiplex PCR method

***Anopheles* species**	**Collection site**				***n***
	Province	**Coordinate**	**Elevation**	**Region**	
An. dissidens	Kanchanaburi	14°07'47.4"N, 98°59'46.0"E	211.4 m	Western Thailand	10
	Narathiwat	6°21'19.3"N, 101°53'41.6"E	9.3 m	Southern Thailand	13
	Trat	12°28'19.7"N 102°40'10.3"E	44.0 m	Eastern Thailand	7
	Total				30
An. saeungae	Kanchanaburi	14°07'47.4"N, 98°59'46.0"E	211.4 m	Western Thailand	9
	Narathiwat	6°21'19.3"N, 101°53'41.6"E	9.3 m	Southern Thailand	15
	Trat	12°28'19.7"N 102°40'10.3"E	44.0 m	Eastern Thailand	6
	Total				30
An. wejchoochotei	Kanchanaburi	14°07'47.4"N, 98°59'46.0"E	211.4 m	Western Thailand	25
	Narathiwat	6°21'19.3"N, 101°53'41.6"E	9.3 m	Southern Thailand	9
	Trat	12°28'19.7"N 102°40'10.3"E	44.0 m	Eastern Thailand	12
	Total				46
An. hodgkini	Kanchanaburi	14°07'47.4"N, 98°59'46.0"E	211.4 m	Western Thailand	6
	Trat	12°28'19.7"N 102°40'10.3"E	44.0 m	Eastern Thailand	24
	Total				30

Note: BG-Pro CDC-style traps (BioGents, Regensburg, Germany) were deployed at each site for 14 consecutive nights to collect *Anopheles* mosquitoes. All specimens belonging to the *An. barbirostris* complex and sister species collected during the sampling period were included in this study

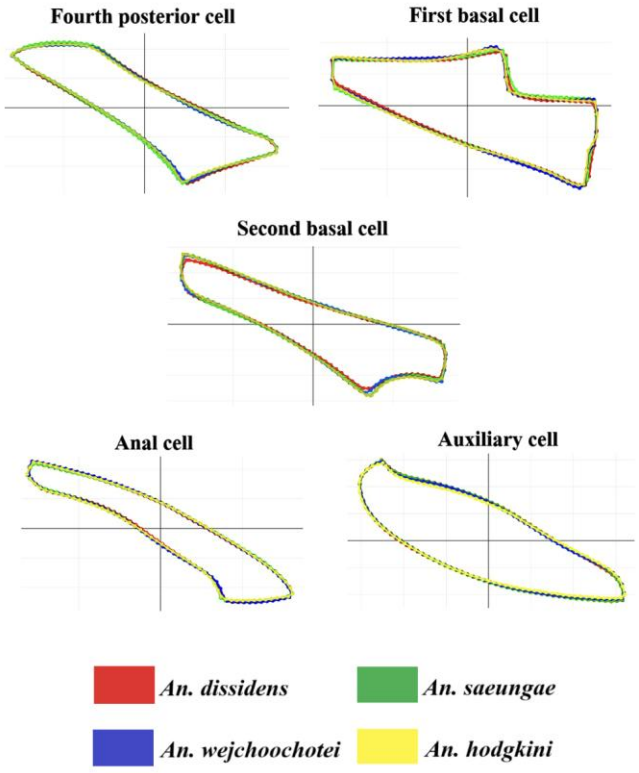

Figure 4. Superimposed mean wing cell shapes illustrating interspecific differences among *An. dissidens, An. saeungae*, *An. wejchoochotei,* and *An. hodgkini* across five wing cells: the fourth posterior cell, first and second basal cells, the anal cell, and the auxiliary cell. Each colored outline represents the mean shape of a species: red for *An. dissidens*, green for *An. saeungae*, blue for *An. wejchoochotei*, and yellow for *An. hodgkini*. The degree of overlap between the outlines reflects interspecific variation in wing cell shape. Although all cells display some degree of morphological divergence, the differences are generally modest

Discussion

Accurate identification of *Anopheles* mosquitoes is critically important for effective malaria surveillance and control (Zhang et al. 2018). Different species exhibit distinct behaviors, such as host preference, biting time, breeding site selection, and vectorial capacity, all of which influence disease transmission dynamics (Sumruayphol et al. 2020). The detection of primary malaria vector species in a given area indicates a potential risk for disease outbreaks (Sumruayphol et al. 2020). Misidentification, particularly within morphologically similar groups such as the *An. barbirostris* complex can lead to inaccurate surveillance data and misguided control efforts.

In this study, molecular classification of mosquito species within the *An. barbirostris* complex confirmed the presence of *An. dissidens*, *An. saeungae*, *An. wejchoochotei*, and the closely related sister species *An. hodgkini*. These findings are consistent with previous reports that members of the complex are morphologically similar and often difficult to distinguish using conventional methods (Wilai et al. 2020). As such, molecular tools, especially multiplex PCR, remain essential for accurate species discrimination (Wilai et al. 2020). Although *An. hodgkini* was previously considered part of the complex (formerly species A3), it is now classified within the *An. barbirostris* group (Somboon et al. 2023). Nevertheless, field identification of *An. hodgkini* remains challenging, and the species is frequently misclassified as a complex member. The present study reinforces the value of species-specific primers developed in earlier research for reliably distinguishing *An. hodgkini* (Wilai et al. 2020).

The vectorial roles of *An. dissidens*, *An. saeungae*, and *An. hodgkini* remains unclear, whereas *An. wejchoochotei* is increasingly recognized as a potential malaria vector in Thailand (Somboon et al. 2023). Differentiating between vector and non-vector species is critical for accurate malaria risk assessments and targeted control strategies. This study also demonstrates the sympatric occurrence of

three *An. barbirostris* complex species and one related taxon across several regions in Thailand. Given their morphological similarity and epidemiological relevance, reliable identification is crucial for effective vector surveillance and malaria control (Davidson et al. 2020). Continued refinement of diagnostic tools is therefore necessary to overcome persistent taxonomic challenges (Nolte et al. 2025).

Superimpositions of mean wing cell shapes revealed distinct differences among *An. dissidens, An. saeungae*, *An. wejchoochotei*, and *An. hodgkini*. These results are consistent with previous studies indicating that curvature in specific anatomical structures may represent species-specific traits, which can be effectively captured using an outline-based GM approach (Dujardin et al. 2014). Traditionally, GM analyses have focused on wing vein intersection points as landmarks to assess interspecific variation in winged insects, a method commonly referred to as landmark-based GM (Kaba et al. 2017; Lorenz et al. 2017; Laojun et al. 2023a, b). However, because insect wings are composed of enclosed regions, known as wing cells, formed by intersecting veins, their shapes are also likely influenced by underlying genetic factors (Dujardin et al. 2014). Detecting such subtle variation requires outline-based GM technique (Samung et al. 2022). Recent studies have proposed that these internal cells may carry latent taxonomic signals in mosquitoes (Laojun et al. 2024). Nevertheless, the utility of wing cell shape for species classification depends on whether the observed variation is sufficiently pronounced to allow reliable discrimination, particularly among closely related or morphologically similar taxa.

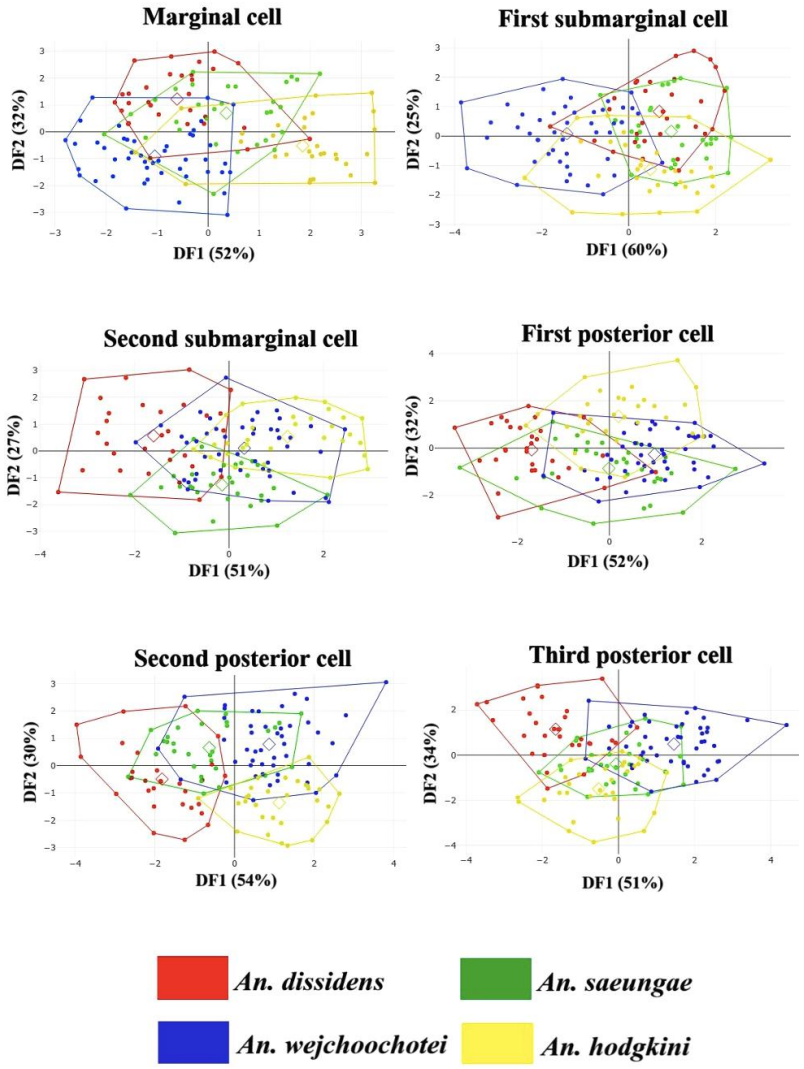

Figure 5. Factor maps based on the first two Discriminant Functions (DF1 on the horizontal axis and DF2 on the vertical axis), derived from final shape variables, illustrating variation in six wing cells: the marginal cell, first and second submarginal cells, and first to third posterior cells, among *An. dissidens, An. saeungae, An. wejchoochotei*, and *An. hodgkini*. Sample sizes are as follows: *An. dissidens* (*n:* 30), *An. saeungae* (*n*: 30), *An. wejchoochotei* (*n*: 46), and *An. hodgkini* (*n:* 30). Colored posterior polygons represent the spatial distribution of each species: red for *An. dissidens*, green for *An. saeungae*, blue for *An. wejchoochotei*, and yellow for *An. hodgkini*. Squares indicate the mean shape position of each species within the discriminant space. Although none of the species forms a distinctly separated cluster, the groups do not fully overlap, as indicated by the distinct positions of their mean shapes

Factor maps highlight morphological variation in the wing cell structures of the four *Anopheles* species. Although the overall wing cell shapes appear highly similar among species, a latent taxonomic signal remains detectable. This is supported by the Mahalanobis distances, which indicate statistically significant shape differences between species. These results align with previous research conducted in Thailand, which analyzed wing shapes of*Aedes aegypti, Ae. albopictus,* and *Ae. scutellaris* using discriminant analysis. That study also detected species-level shape differences, though with a high degree of overlap among groups as revealed by DA (Chonephetsarath et al. 2021).

Mahalanobis distance-based pairwise comparisons revealed statistically significant differences (p<0.05) in wing cell shape among most species pairs, across nearly all examined cells. These statistical differences in wing cell shape reflect species-specific morphological traits influenced by underlying genetics and can be interpreted as evidence of the taxonomic signal (Chonephetsarath et al. 2021). The pronounced divergence observed in *An. hodgkini*, as indicated by its consistently high Mahalanobis distances, probably results from its confirmed genetic separation from the *An. barbirostris* complex—despite previous classifications that included it within the complex (Somboon et al. 2023). In contrast, *An. dissidens, An. saeungae,* and *An. wejchoochotei* are phylogenetically closer, as recognized members of the *An. barbirostris* complex, which explains the greater similarity observed in their wing cell shapes (Somboon et al. 2023).

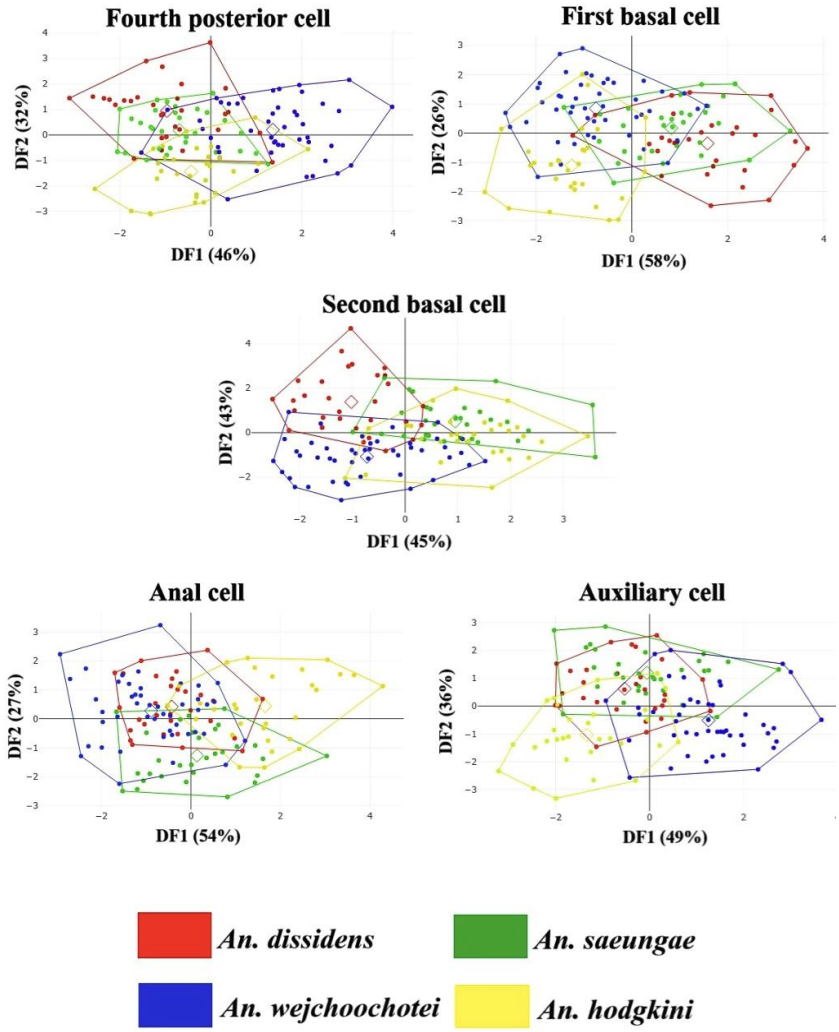

Figure 6. Factor maps based on the first two Discriminant Functions (DF1 on the horizontal axis and DF2 on the vertical axis), derived from final shape variables, illustrating variation in five wing cells: the fourth posterior cell, first and second basal cells, the anal cell, and the auxiliary cell, among *An. dissidens, An. saeungae, An. wejchoochotei*, and *An. hodgkini*. Sample sizes are as follows: *An. dissidens* (*n:* 30), *An. saeungae* (*n*: 30), *An. wejchoochotei* (*n*: 46), and *An. hodgkini* (*n:* 30). Colored posterior polygons represent the spatial distribution of each species: red for *An. dissidens*, green for *An. saeungae*, blue for *An. wejchoochotei*, and yellow for *An. hodgkini*. Squares indicate the mean shape position of each species within the discriminant space. Although none of the species forms a distinctly separated cluster, the groups do not fully overlap, as indicated by the distinct positions of their mean shapes

Although several statistically significant differences in wing cell shapes were detected among *An. dissidens, An. saeungae, An. wejchoochotei*, and *An. hodgkini*, the overall performance of cross-validated classification remained moderate and may not be sufficiently robust for practical species identification in field settings. This result likely reflects the high morphological similarity among these taxa, which are genetically close and classified as sibling species or closely related members of the *An. barbirostris* complex. Furthermore, when compared to a previous study that employed a landmark-based GM approach to analyze overall wing structure for species classification within the *An. barbirostris* complex in Thailand, wing cell-based classification was found to be less effective (74.29% vs. 44.12-58.09%) (Chaiphongpachara et al. 2022b). This suggests that using the entire wing structure yields more reliable discrimination than relying on individual wing cells.

From a genetic perspective, previous studies using mitochondrial *COI* and nuclear ITS2 markers have confirmed that *An. hodgkini* forms a distinct clade, genetically distant from *An. dissidens, An. saeungae,* and *An. wejchoochotei* (Somboon et al. 2023). This phylogenetic separation aligns with the morphometric results observed in the present study, particularly in the second posterior, marginal, and first basal cells, indicating that wing shape may serve as a phenotypic marker for cryptic genetic divergence. Conversely, the significant overlap in wing morphology between *An. dissidens* and *An. wejchoochotei*, especially in the anal cell, matches their closer genetic relationship and shared ecological niches.

In addition, a comparison with the findings of a previous study on *Anopheles* wing cell shape analysis conducted in the Tanaosri mountain range, Thailand, revealed that the third posterior cell was highly effective in distinguishing seven species *(An. dravidicus, An. maculatus, An. minimus, An. paraliae, An. sawadwongporni, An. subpictus*, and *An. wejchoochotei),* achieving an overall classification accuracy of 84.58% (ranging from 72.73% to 96.88%; Laojun et al. 2024). In contrast, the present study found that the third posterior cell exhibited only moderate discriminatory power in differentiating species within the *An. barbirostris* complex, with an overall accuracy of 56.62% (ranging from 36.67% to 63.33%). This discrepancy suggests that species within the *An. barbirostris* complex is more morphologically similar to one another, making species delimitation based solely on wing cell shape more difficult. Therefore, although wing cell morphology contains latent taxonomic signals and demonstrates moderate discriminative capacity, it is insufficient on its own for precise species identification. For accurate and reliable classification within this *Anopheles* complex, molecular methods remain essential and continue to represent the gold standard.

Table 3. Significant differences in the shape of each wing cell among *An. dissidens, An. saeungae, An. wejchoochotei,* and *An. hodgkini*, based on Mahalanobis distances

Species	*An. dissidens*	*An. saeungae*	*An. wejchoochotei*	*An. hodgkini*
Marginal cell (below diagonal) / First submarginal cell (above diagonal)				
An. dissidens	-	1.605	2.361*	2.002*
An. saeungae	2.047*	-	2.504*	1.791*
An. wejchoochotei	2.295*	2.344*	-	2.310*
An. hodgkini	3.029*	2.390*	2.957*	-
Second submarginal cell (below diagonal) / First posterior cell (above diagonal)				
An. dissidens	-	2.210*	2.671*	2.471*
An. saeungae	2.332*	-	1.739*	2.259*
An. wejchoochotei	2.280*	1.873*	-	1.973*
An. hodgkini	2.874*	2.307*	1.898*	-
Second posterior cell (below diagonal) / Third posterior cell (above diagonal)				
An. dissidens	-	2.607*	3.174*	2.907*
An. saeungae	2.266*	-	2.263*	2.132*
An. wejchoochotei	2.977*	2.121*	-	2.824*
An. hodgkini	3.171*	2.775*	2.277*	-
Fourth posterior cell (below diagonal) / First basal cell (above diagonal)				
An. dissidens	-	1.896*	2.648*	3.017*
An. saeungae	2.094*	-	2.123*	2.613*
An. wejchoochotei	2.544*	2.380*	-	2.042*
An. hodgkini	2.471*	2.243*	2.448*	-
Second basal cell (below diagonal) / Anal cell (above diagonal)				
An. dissidens	-	1.991*	1.582	2.389*
An. saeungae	2.366*	-	1.950*	2.302*
An. wejchoochotei	2.504*	2.385*	-	2.573*
An. hodgkini	2.767*	1.621*	2.243*	-
Auxiliary cell				
An. dissidens	-			
An. saeungae	1.794	-		
An. wejchoochotei	2.295*	2.276*	-	
An. hodgkini	2.207*	2.604*	2.662*	-

Note: The values in the table represent Mahalanobis distances, which quantify the geometric divergence in wing cell shape between pairs of species. Higher values indicate greater differences. An asterisk (*) denotes statistically significant differences at $p<0.05$

Table 4. Cross-validated reclassification accuracies (percentages) of each *Anopheles* species based on individual wing cells

Wing cell	% reclassification (Correctly assigned/total investigated individuals)				
	An. dissidens	*An. saeungae*	*An. wejchoochotei*	*An. hodgkini*	Total
Marginal cell	50.00% (15/30)	40.00% (12/30)	58.70% (27/46)	66.67% (20/30)	54.41% (74/136)
First submarginal cell	36.67% (11/30)	43.33% (13/30)	56.52% (26/46)	46.67% (14/30)	47.06% (64/136)
Second submarginal cell	56.67% (17/30)	40.00% (12/30)	45.65% (21/46)	60.00% (18/30)	50.00% (68/136)
First posterior cell	63.33% (19/30)	30.00% (9/30)	45.65% (21/46)	53.33% (16/30)	47.79% (65/136)
Second posterior cell	63.33% (19/30)	40.00% (12/30)	60.87% (28/46)	66.67% (20/30)	58.09% (79/136)
Third posterior cell	60.00% (18/30)	36.67% (11/30)	63.04% (29/46)	63.33% (19/30)	56.62% (77/136)
Fourth posterior cell	56.67% (17/30)	50.00% (15/30)	63.04% (29/46)	53.33% (16/30)	56.62% (77/136)
first basal cell	50.00% (15/30)	43.33% (13/30)	52.17% (24/46)	63.33% (19/30)	52.21% (71/136)
Second basal cell	56.67% (17/30)	36.67% (11/30)	58.70% (27/46)	40.00% (12/30)	49.26% (67/136)
Anal cell	43.33% (13/30)	43.33% (13/30)	43.48% (20/46)	46.67% (14/30)	44.12% (60/136)
Auxiliary cell	36.67% (11/30)	53.33% (16/30)	56.52% (26/46)	63.33% (19/30)	52.94% (72/136)

The relationship between mosquito morphology and vector competence has been increasingly emphasized in entomological and epidemiological studies (Alto et al. 2008; Lorenz et al. 2017). Previous research suggests that larger mosquito body size is positively associated with vectorial capacity, as bigger individuals typically exhibit longer lifespans, greater blood-feeding success, and enhanced survivability—all of which contribute to a higher probability of acquiring and transmitting pathogens (Alto et al. 2008; Phasomkusolsil et al. 2015). Moreover, larger mosquitoes often ingest greater blood volumes, thereby increasing their chances of becoming infected when feeding on a parasitemic host (Alto et al. 2008). Simultaneously, variation in wing shape plays a pivotal role in biological functions such as flight efficiency, dispersal capacity, and host-seeking behavior (Lorenz et al. 2017; Krishna et al. 2020). Subtle differences in wing cell contours can affect aerodynamic performance, which in turn influences how mosquitoes locate and access hosts or breeding sites. For instance, the wings that are more elongated or broader may facilitate long-distance dispersal or improve maneuverability in dense environments, thereby affecting interactions with human or animal hosts. From a vector surveillance and malaria control perspective, these morphological traits—especially when associated with specific cryptic species or ecological adaptations—can influence local transmission dynamics. Identifying and characterizing these traits not only improves taxonomic resolution but also enhances the ability to predict vector behavior, distribution patterns, and transmission risk (Champakaew et al. 2021; Sauer et al. 2023). These insights are essential for designing targeted and effective control strategies, particularly in regions with high species diversity and limited access to molecular diagnostic tools.

In conclusion, this study underscores the practical usefulness and biological significance of GM in distinguishing cryptic malaria vector species within the *An. barbirostris* complex and its sister species, *An. hodgkini*. The findings demonstrate that wing cell shape variation—particularly in the second posterior, marginal, and auxiliary cells—offers valuable morphological signals capable of distinguishing species with similar external features. *Anopheles hodgkini* exhibited the highest reclassification accuracy across several wing cells, reaching up to 66.67%, reflecting its pronounced morphological differences from the other species. Conversely, *An. saeungae* consistently yielded lower classification rates, illustrating the difficulty of discriminating among morphologically similar, sympatric species based solely on wing shape. From both taxonomic and public health perspectives, GM offers a cost-effective, rapid, and field-friendly method for vector monitoring. Unlike molecular techniques, GM requires minimal laboratory infrastructure and can be applied retrospectively to archived specimens, including slide-mounted wings or museum collections. This makes it especially advantageous for long-term monitoring efforts in resource-constrained settings with limited access to DNA-based diagnostics. Nevertheless, GM has inherent limitations—particularly in resolving species with strong morphological convergence—highlighting the need for an integrative approach. A combined molecular-morphological framework is recommended. GM can serve as a prescreening tool to identify specimens with atypical shapes, which can then undergo confirmatory testing via multiplex PCR. This integrative strategy enhances taxonomic accuracy and offers deeper ecological interpretations by linking morphological traits to genetic lineages and environmental factors. Overall, the insights gained from this study support the broader application of GM in biodiversity assessment, species delimitation, and entomological surveillance. In regions where cryptic vectors co-occur, morphometric analysis can contribute to spatial risk modeling, refine epidemiological predictions, and support the development of species-specific vector control strategies. Future research should prioritize the expansion of GM reference databases and integration with molecular phylogenetics to advance our understanding of vector adaptation.

ACKNOWLEDGEMENTS

This research was supported by the National Science, Research, and Innovation Fund (NSRF) through Suan Sunandha Rajabhat University, Thailand. The authors express their sincere gratitude to all individuals who contributed to this study, including research assistants and local collaborators, whose assistance in field sample collection was invaluable. We are grateful to Professor Pradya Somboon for providing valuable information about the *Anopheles barbirostris* complex.

REFERENCES

Alto BW, Reiskind MH, Lounibos LP, 2008. Size alters susceptibility of vectors to dengue virus infection and dissemination. Am J Trop Med Hyg 79: 688-695. DOI: 10.4269/ajtmh.2008.79.688.

Arnqvist G, Mårtensson T, 1998. Measurement error in geometric morphometrics: empirical strategies to assess and reduce its impact on measures of shape. Acta Zool Acad Sci Hung 44: 73-96.

Bellin N, Calzolari M, Callegari E, Bonilauri P, Grisendi A, Dottori M, Rossi V. 2021. Geometric morphometrics and machine learning as tools for the identification of sibling mosquito species of the Maculipennis complex (*Anopheles*). Infect Genet Evol 95: 105034. DOI: 10.1016/j.meegid.2021.105034.

Chaiphongpachara T, Changbunjong T, Laojun S. 2022b. Geometric morphometric and molecular techniques for discriminating among three cryptic species of the *Anopheles barbirostris* complex (Diptera: Culicidae) in Thailand. Heliyon 8: e11261. DOI: 10.1016/j.heliyon.2022.e11261.

Chaiphongpachara T, Changbunjong T, Sumruayphol S, Laojun S, Suwandittakul N, Kuntawong K. 2022a. Geometric morphometrics versus DNA barcoding for the identification of malaria vectors *Anopheles dirus* and *An. baimaii* in the Thai-Cambodia border. Sci Rep 12: 13236. DOI: 10.1038/s41598-022-17646-6.

Champakaew D, Junkum A, Sontigun N, Sanit S, Limsopatham K, Saeung A, Somboon P, Pitasawat B. 2021. Geometric morphometric wing analysis as a tool to discriminate female mosquitoes from different suburban areas of Chiang Mai province, Thailand. Plos One 16: e0260333. DOI: 10.1371/journal.pone.0260333.

Changbunjong T, Weluwanarak T, Laojun S, Chaiphongpachara T. 2025. Species classification of *Tabanus* (Diptera: Tabanidae) in Western Thailand: Integrating DNA barcoding and modern morphometrics. Curr Res Parasitol Vector-Borne Dis 7: 100243. DOI: 10.1016/j.crpvbd.2025.100243.

Chatpiyaphat K, Sumruayphol S, Dujardin JP, Samung Y, Phayakkaphon A, Cui L, Ruangsittichai J, Sungvornyothin S, Sattabongkot J,

Sriwichai P. 2021. Geometric morphometrics to distinguish the cryptic species *Anopheles minimus* and *An. harrisoni* in malaria hot spot villages, western Thailand. Med Vet Entomol 35: 293-301. DOI: 10.1111/mve.12493.

Chonephetsarath S, Raksakoon C, Dujardin JP. 2021. The unequal taxonomic signal of mosquito wing cells. Insects 12 (5): 376. DOI: 10.3390/insects12050376.

Chotelersak K, Puttikamonkul S, Samung Y, Chaiphongpachara T, Dujardin JP, Sumruayphol S. 2024. *Ctenocephalides orientis* and *Ctenocephalides felis* in Thailand: Head geometry by species, sex and geography. Med Vet Entomol 38: 179-188. DOI: 10.1111/mve.12707.

Davidson JR, Wahid I, Sudirman R, Small ST, Hendershot AL, Baskin RN, Burton TA, Makuru V, Xiao H, Yu X, Troth EV, Olivieri D, Lizarraga S, Hasan H, Arfah A, Yusuf M, Nur N, Syafruddin D, Asih P, Lobo NF. 2020. Molecular analysis reveals a high diversity of Anopheles species in Karama, West Sulawesi, Indonesia. Parasit Vectors 13: 379. DOI: 10.1186/s13071-020-04252-6.

de Souza ALDS, Multini LC, Marrelli MT, Wilke ABB. 2020. Wing geometric morphometrics for identification of mosquito species (Diptera: Culicidae) of neglected epidemiological importance. Acta Trop 211: 105593. DOI: 10.1016/j.actatropica.2020.105593.

Dujardin J, Kaba D, Solano P, Dupraz M, Mccoy KD, Jaramillo-o N. 2014. Outline-based morphometrics, an overlooked method in arthropod studies? Infect Genet Evol 28: 704-714. DOI: 10.1016/j.meegid.2014.07.035.

Dujardin S, Dujardin JP. 2019. Geometric morphometrics in the cloud. Infect Genet Evol 70: 189-196. DOI: 10.1016/j.meegid.2019.02.018.

Jeon J, Kim HC, Klein TA, Choi KS. 2023. Analysis of geometric morphometrics and molecular phylogeny for *Anopheles* species in the Republic of Korea. Sci Rep 13: 22009. DOI: 10.1038/s41598-023-49536-w.

Kaba D, Berté D, Ta BTD, Tellería J, Solano P, Dujardin J. 2017. The wing venation patterns to identify single tsetse flies. Infect Genet Evol 47: 132-139. DOI: 10.1016/j.meegid. 2016.10.008.

Krishna S, Cho M, Wehmann HN, Engels T, Lehmann FO. 2020. Wing design in flies: Properties and aerodynamic function. Insects 11 (8): 466. DOI: 10.3390/insects11080466.

Laojun S, Changbunjong T, Chaiphongpachara T. 2023a. Evaluation of modern techniques for species identification of *Lutzia* mosquitoes (Diptera: Culicidae) in Thailand: Geometric morphometrics and DNA barcoding. Insects 14 (1): 78. DOI: 10.3390/insects14010078.

Laojun S, Changbunjong T, Sumruayphol S, Chaiphongpachara T. 2023b. Molecular and morphometric differentiation of secondary filariasis vector *Coquillettidia* mosquitoes (Diptera: Culicidae) in Thailand. Infect Genet Evol 112: 105452. DOI: 10.1016/ j.meegid.2023.105452.

Laojun S, Changbunjong T, Sumruayphol S, Chaiphongpachara T. 2024. Outline-based geometric morphometrics: Wing cell differences for mosquito vector classification in the Tanaosri mountain range, Thailand. Acta Trop 250: 107093. DOI: 10.1016/j.actatropica. 2023.107093.

Lorenz C, Almeida F, Almeida-Lopes F, Louise C, Pereira SN, Petersen V, Vidal PO, Virginio F, Suesdek L. 2017. Geometric morphometrics in mosquitoes: What has been measured? Infect Genet Evol 54: 205-215. DOI: 10.1016/j.meegid.2017.06.029.

Lozano-Sardaneta YN, Mikery-Pacheco OF, Huerta H, Rojas-Soriano JE, Contreras-Ramos A. 2025. Wing geometric morphometrics is effective to separate sand fly species (Diptera, Psychodidae, Phlebotominae) related with leishmaniasis transmission in Mexico. Acta Trop 262: 107523. DOI: 10.1016/j.actatropica.2025.107523.

Nguyen AHL, Pattaradilokrat S, Kaewlamun W, Kaneko O, Asada M, Kaewthamasorn M. 2023. Myzomyia and Pyretophorus series of *Anopheles* mosquitoes acting as probable vectors of the goat malaria parasite *Plasmodium caprae* in Thailand. Sci Rep 13: 145. DOI: 10.1038/s41598-022-26833-4.

Nolte K, Agboli E, Garcia GA et al. 2025. Comprehensive mosquito wing image repository for advancing research on geometric morphometric- and AI-based identification. Sci Data 12: 715. DOI: 10.1038/s41597-025-05043-3.

Oliveira-Christe R, de Carvalho GC, Wilke ABB, Marrelli MT. 2023. Assessment of wing geometric morphometrics of urban *Culex quinquefasciatus* (Diptera: Culicidae) populations. Acta Trop 245: 106971. DOI: 10.1016/j.actatropica.2023.106971.

Parker DM, Carrara VI, Pukrittayakamee S, McGready R, Nosten FH. 2015. Malaria ecology along the Thailand-Myanmar border. Malar J 14: 388. DOI: 10.1186/s12936-015-0921-y.

Phasomkusolsil S, Pantuwattana K, Tawong J, Khongtak W, Kertmanee Y, Monkanna N, Klein TA, Kim HC, McCardle PW. 2015. The relationship between wing length, blood meal volume, and fecundity for seven colonies of *Anopheles* species housed at the Armed Forces Research Institute of Medical Sciences, Bangkok, Thailand. Acta Trop 152: 220-227. DOI: 10.1016/j.actatropica.2015.09.021.

Rattanarithikul R, Harrison BA, Harbach RE, Panthusiri P, Coleman RE. 2006. Illustrated keys to the mosquitoes of Thailand IV. *Anopheles.* Southeast Asian J Trop Med Publ Health 37 (2): 1-128.

Rotejanaprasert C, Malaphone V, Maysay M, Chindavongsa K, Banouvong V, Khamlome B, Vilay P, Vanisavaeth V, Maude RJ. 2024. Malaria epidemiology, surveillance, and response for elimination in Lao PDR. Infect Dis Poverty 13: 35. DOI: 10.1186/s40249-024-01202-7.

Samung Y, Chaiphongpachara T, Ruangsittichai J, Sriwichai P, Phayakkaphon A, Jaitrong W, Dujardin JP, Sumruayphol S. 2022. Species discrimination of three *Odontomachus* (Formicidae: Ponerinae) species in Thailand using outline morphometrics. Insects 13 (3): 287. DOI: 10.3390/insects13030287.

Santillán-Guayasamín S, Villacís AG, Grijalva MJ, Dujardin JP. 2017. The modern morphometric approach to identify eggs of Triatominae. Parasit Vectors 10: 55. DOI: 10.1186/s13071-017-1982-2.

Sauer FG, Jaworski L, Erdbeer L, Heitmann A, Schmidt-Chanasit J, Kiel E, Lühken R. 2020. Geometric morphometric wing analysis represents a robust tool to identify female mosquitoes (Diptera: Culicidae) in Germany. Sci Rep 10: 17613. DOI: 10.1038/s41598-020-72873-z.

Sauer FG, Pfitzner WP, Jöst H, Rauhöft L, Kliemke K, Lange U, Heitmann A, Jansen S, Lühken R. 2023. Using geometric wing morphometrics to distinguish *Aedes japonicus japonicus* and *Aedes koreicus*. Parasit Vectors 16: 418. DOI: 10.1186/s13071-023-06038-y.

Somboon P, Saeung A, Saingamsook J. 2024. A new species of the *Anopheles barbirostris* complex (Diptera: Culicidae) from Bhutan. J Med Entomol 61 (2): 377-388. DOI: 10.1093/jme/tjad161.

Somboon P, Wilai P, Saeung A, Saingamsook J, Harbach RE. 2023. The identity of *Anopheles (Anopheles) barbirostris* species A3 of the Barbirostris complex (Diptera: Culicidae). Zootaxa 5353: 96-100. DOI: 10.11646/zootaxa.5353.1.8.

Sumruayphol S, Chaiphongpachara T, Samung Y, Ruangsittichai J, Cui L, Zhong D, Sattabongkot J, Sriwichai P. 2020. Seasonal dynamics and molecular differentiation of three natural *Anopheles* species (Diptera: Culicidae) of the Maculatus group (Neocellia series) in malaria hotspot villages of Thailand. Parasit Vectors 13: 574. DOI: 10.1186/s13071-020-04452-0.

Taai K, Harbach RE. 2015. Systematics of the *Anopheles barbirostris* species complex (Diptera: Culicidae: Anophelinae) in Thailand. Zool J Linn Soc 174: 244-264 DOI: 10.1111/zoj.12236.

Tananchai C, Manguin S, Bangs MJ, Chareonviriyaphap T. 2019. Malaria vectors and species complexes in Thailand: Implications for vector control. Trends Parasitol 35: 544-558. DOI: 10.1016/j.pt.2019.04.013.

Udom C, Thanispong K, Manguin S, Chareonviriyaphap T, Fungfuang W. 2021. Trophic behavior and species diversity of the *Anopheles barbirostris* complex (Diptera: Culicidae) in Thailand. J Med Entomol 58: 2376-2384. DOI: 10.1093/jme/tjab067.

Weluwanarak T, Chaiphongpachara T, Changbunjong T. 2024. Evaluation of the wing cell contour to distinguish between *Stomoxys bengalensis* and *Stomoxys sitiens* (Diptera: Muscidae) using outline-based morphometrics. Curr Res Parasitol Vector Borne Dis 6: 100204. DOI: 10.1016/j.crpvbd.2024.100204.

Wilai P, Namgay R, Ali RSM, Saingamsook J, Saeung A, Junkum A, Walton C, Harbach RE, Somboon P. 2020. A multiplex PCR based on mitochondrial *COI* sequences for identification of members of the *Anopheles barbirostris* complex (Diptera: Culicidae) in Thailand and other countries in the region. Insects 11 (7): 409. DOI: 10.3390/insects11070409.

Wilke AB, Christe Rde O, Multini LC, Vidal PO, Wilk-da-Silva R, de Carvalho GC, Marrelli MT. 2016. Morphometric wing characters as a tool for mosquito identification. Plos One 11 (8): e0161643. DOI: 10.1371/journal.pone.0161643.

Zhang SS, Zhou SS, Zhou ZB, Chen TM, Wang XZ, Shi WQ, Jiang WK, Li JL, Zhou XN, Frutos R, Manguin S, Afelt A. 2018. Monitoring of malaria vectors at the China-Myanmar border while approaching malaria elimination. Parasit Vectors 11: 511. DOI: 10.1186/s13071-018-3073-4.